

# Measurement and statistical modeling of BRDF of various samples

HANLU ZHANG, ZHENSEN WU\*, YUNHUA CAO, GENG ZHANG

School of Sciences, Xidian University, Xi'an, Shaanxi, 710071, China

\*Corresponding address: wuzhs@mail.xidian.edu.cn

Based on the Torrance–Sparrow model, a modified and simplified five-parameter model is obtained. Multi-angle bistatic reflectance data of surfaces of various materials are fitted using this model. Genetic algorithm is used to optimize the parameters for the model. The results of the five-parameter model are in good agreement with experimental data which do not take part in fitting, and are close to the results of two-dimensional bidirectional reflectance distribution function (BRDF) models. The five-parameter model shows a good applicability to various rough surfaces with different surface optical properties. The five-parameter model can be used to construct a three-dimensional BRDF distribution based on the spatial experimental data, which may provide more information on light scattering from rough surfaces.

Keywords: bidirectional reflectance distribution function (BRDF), modeling, measurement, light scattering.

## 1. Introduction

Scattering of rough surfaces, conducting or dielectric targets, has been widely studied in the microwave band [1–6]. But it is difficult to study scattering of targets in the visible band because the wavelength is too short to use the classical electromagnetic theory. Bidirectional reflectance distribution function (BRDF) defined by NICODEMUS [7], which is a theoretical concept that describes the directional reflectance phenomena by relating the incident radiance from one given direction to its contribution to the reflected radiance in another specific direction, makes the calculation of light scattering of targets more easily [8]. BRDF is now extensively used in the fields of remote sensing and material diagnosis for characterization of light radiation and scattering from surfaces [9–12]. BRDF plays a major role in evaluating or simulating the signatures of natural and artificial targets in the visible spectrum using a laser [13–17]. Various surface BRDF models [18–22], plus theory and measurements of the polarized BRDF, have been developed [23–27]. Usually, a large amount of BRDF data is needed to fully characterize three-dimensional light scattering from an object surface [28], which might not be experimentally realizable in practice. Therefore,

an effective model founded on limited experimental data is required to efficiently obtain light scattering information.

In 1967 TORRANCE and SPARROW deduced a light scattering model [29], which assumes that the surface consists of small, randomly disposed, mirror-like facets. The model can predict the off-specular peak phenomenon caused by masking and shadowing of surface facets, but it restricts the distribution of the normal of the mirror-like facets being Gaussian. Based on TS model, we proposed a five-parameter model. In this model, the exponential function in the TS model is substituted by elliptical function to describe the distribution of the normal of the facets. In addition, the exponential function with two parameters is used to substitute the Fresnel reflectance function to avoid the calculation of many trigonometric functions. The model can be used to describe the isotropic surfaces with non-polarization incident light. The model is simpler in calculation procedure and wider in applied ranges, so it is more applicable than the TS model.

Genetic algorithm [30], which is an adaptive and probability optimizing algorithm originating from simulation of hereditary and evolutionary progress of the organism in environment, is used to search the best parameters of the five-parameter BRDF model to fit the measured data. And BRDF calculated using the model with the retrieved parameters can fit the measured data well.

Several isotropic samples with different light scattering characters are measured, and the five-parameter model is used to fit the experimental data. It is found that the model is successful in fitting these data.

## 2. Establishment of five-parameter BRDF statistical model

In optical and infrared fields, if the microscopic roughness scale is much larger than that of radiation wavelength ( $k\sigma > 1$ , while  $k$  is the wave number,  $\sigma$  is the roughness scale), rough surfaces can be considered as made of many facets with normal pointing to space [29]. The coordinate system is shown in Fig. 1. Let us assume that the  $z$  axis is normal to the averaged plane of the rough surface,  $\mathbf{k}_i$  is the incident vector,  $\mathbf{k}_r$  is

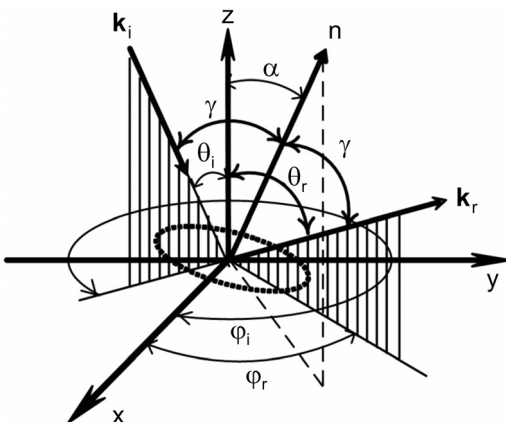


Fig. 1. Diagram showing the geometric relation of BRDF in Cartesian coordinate.

the scattered vector,  $\alpha$  is the angle between the normal direction  $\mathbf{n}$  of the facet and the  $z$  axis,  $\gamma$  is the incident angle in the local coordinate of the facet. The relationship between  $\alpha$  and  $\gamma$  in a rectangular coordinate system is (assume  $\varphi_i = 0$ )

$$\left. \begin{aligned} \cos \alpha &= \frac{\cos \theta_i + \cos \theta_r}{2 \cos \gamma} \\ \cos^2 \gamma &= \frac{1}{2} (\cos \theta_i \cos \theta_r + \sin \theta_i \sin \theta_r \cos \varphi_r + 1) \end{aligned} \right\} \quad (1)$$

where:  $r$  – reflected,  $i$  – incident,  $\theta$  – zenith angle,  $\varphi$  – azimuth angle. Based on this, Torrance and Sparrow deduced a light model from a rough surface. The model assumes that the surface consists of small, mirror-like facets which follow the Gaussian probability distribution. The effects of shadowing and masking of facets by adjacent facets are included in the analysis. The TS (Torrance and Sparrow) model is

$$f_r(\theta_i, \varphi_i, \theta_r, \varphi_r) = gR(\gamma, n) \frac{G(\theta_i, \varphi_i, \theta_r, \varphi_r)}{\cos \theta_r} \exp(-C^2 \alpha^2) + \frac{\rho_0}{\pi} \cos \theta_i \quad (2)$$

The model is composed of two components: the coherent component – specular reflection, and the Lambert component – diffuse reflection. The  $g$  denotes the adjustable constant;  $R(\gamma, n)$  is the Fresnel reflection function;  $G(\theta_i, \varphi_i, \theta_r, \varphi_r)$  is the masking and shadowing factor;  $C$  is the parameter controlling the spread of the facet distribution;  $\rho_0$  is the diffuse reflectance.

In the TS model, the distribution function of the normal of the facet is Gaussian in the expression of  $D = \exp(-C^2 \alpha^2)$ . As to isotropic surface, the distribution of the normal of the facet is symmetrical in azimuth to the normal of the reflected surface, so the exponential function in the TS model is substituted by the elliptical function  $D(\alpha) = k_r^2 \cos \alpha / [1 + (k_r^2 - 1) \cos^2 \alpha]$ . The coefficient  $k_r$  is the ratio of the horizontal axis to the vertical axis. The specular peak is more predominant, and the value of  $k_r$  is smaller.

As to isotropic surface incident with non-polarized light, Fresnel reflectance coefficient can be approximated by an exponential function with two parameters  $R_0(\gamma) = \exp[b(1 - \cos \gamma)^a]$ .  $R_0(\gamma)$  is the relative reflection coefficient of the facet  $R_0(\gamma) = R(\gamma)/R(0)$ ;  $a, b$  are determined by the refractive index of medium. When  $R_0(\pi/2) = R(\pi/2)/R(0) = \exp(b) = (n + 1)^2/(n - 1)^2$ , the initial value of  $b$  can be taken  $b = \ln[(n + 1)/(n - 1)]^2$ , here  $n$  is the refractive index of medium. The expression can save a lot of calculation time consumed by the calculation of many trigonometric functions in the classical expression of Fresnel reflectance function.

The shadowing function  $G(\theta_i, \theta_r, \varphi_r)$  is determined by the probability of shadowing and masking, which occurred between the adjacent facets. In order to simplify the formula, the microgeometric model is introduced (as shown in Fig. 2).

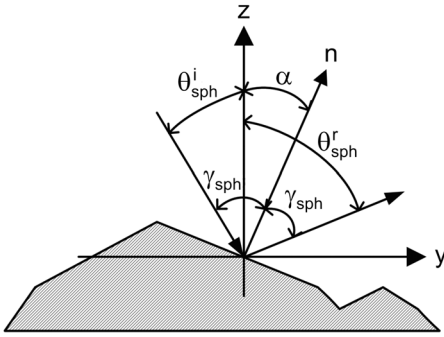


Fig. 2. Diagram showing the microgeometric model of BRDF in two-dimensional coordinate.

The  $\theta_{\text{sph}}^i$ ,  $\theta_{\text{sph}}^r$  and  $\gamma_{\text{sph}}$  are the projection of  $\theta_i$ ,  $\theta_r$  and  $\gamma$ , respectively in the scattering plane. Based on this, the shadowing function can be written as

$$G(\theta_i, \theta_r, \varphi_r) = \frac{1 + w_{\text{sph}}(\alpha) |\tan \theta_{\text{sph}}^i \tan \theta_{\text{sph}}^r| / (1 + \sigma_r \tan \gamma_{\text{sph}})}{\left[1 + w_{\text{sph}}(\alpha) \tan^2 \theta_{\text{sph}}^i\right] \left[1 + w_{\text{sph}}(\alpha) \tan^2 \theta_{\text{sph}}^r\right]} \quad (3)$$

where:  $w_{\text{sph}}(\alpha) = \sigma_{\text{sph}} [1 + u_{\text{sph}} \sin \alpha / (\sin \alpha + v_{\text{sph}} \cos \alpha)]$ , and  $\sigma_r$ ,  $\sigma_{\text{sph}}$ ,  $u_{\text{sph}}$ ,  $v_{\text{sph}}$  are the empirical parameters. In general, these parameters can be obtained by many experiments. In this paper, we let  $\sigma_{\text{sph}} = 0.0136$ ,  $\sigma_r = 0.0141$ ,  $u_{\text{sph}} = 9.0$ ,  $v_{\text{sph}} = 1.0$ , then the function can calculate the geometrical attenuation factor of the flux.

According to the spherical trigonometry formulas, the tangent functions of  $\theta_{\text{sph}}^i$ ,  $\theta_{\text{sph}}^r$  and  $\gamma_{\text{sph}}$ , and are

$$\left. \begin{aligned} \tan \theta_{\text{sph}}^i &= \tan \theta_i \frac{\sin \theta_i + \sin \theta_r \cos \varphi_r}{2 \sin \alpha \cos \gamma} \\ \tan \theta_{\text{sph}}^r &= \tan \theta_r \frac{\sin \theta_r + \sin \theta_i \cos \varphi_r}{2 \sin \alpha \cos \gamma} \\ \tan \gamma_{\text{sph}} &= \frac{|\cos \theta_i - \cos \gamma|}{2 \sin \alpha \cos \gamma} \end{aligned} \right\} \quad (4)$$

Based on all of the above equations, the BRDF model can be written as five-parameter ( $k_b$ ,  $k_r$ ,  $a$ ,  $b$  and  $k_d$ ) model:

$$f_r(\theta_i, \theta_r, \varphi_r) = k_b \frac{k_r^2 \cos \alpha}{1 + (k_r^2 - 1) \cos \alpha} \exp \left[ b(1 - \cos \gamma)^a \right] \frac{G(\theta_i, \theta_r, \varphi_r)}{\cos \theta_r} + k_d \quad (5)$$

while  $k_b$  is the specular reflection coefficient,  $k_d$  is the diffuse reflection coefficient.

The best standard to select parameters is the least square error criterion. So the objective function is given by:

$$E(x) = \frac{\sum_{\theta_i} \sum_{\theta_r} g_1(\theta_i) g_2(\theta_r) \left[ f_r(\theta_i, \theta_r, 0) \cos \theta_r - f_r^0(\theta_i, \theta_r, 0) \cos \theta_r \right]^2}{\sum_{\theta_i} \sum_{\theta_r} g_1(\theta_i) g_2(\theta_r) \left[ f_r^0(\theta_i, \theta_r, 0) \cos \theta_r \right]^2} \quad (6)$$

where:  $x = [k_b, k_d, k_r, a, b]^T$  is the column vector of experimental parameters;  $f_r(\theta_i, \theta_r, 0)$  and  $f_r^0(\theta_i, \theta_r, 0)$  are the value of BRDF calculated using Eq. (5) and the measured data of BRDF at  $(\theta_i, \theta_r, 0)$ , respectively;  $g_1(\theta_i)$  and  $g_2(\theta_r)$  are the weighting functions to adjust errors induced by nonuniform measurement, rendering the results more exact through appropriate employment. In this paper the weighting functions are set as 1.

### 3. Experimental method

BRDF of samples is measured using the measurement system (designed and built by Anhui Institute of Optics and Fine Mechanics, Chinese Academy of Sciences) shown in Fig. 3. The system can measure three dimensional BRDF data by rotating the sample and the light source by motors A, B and C. The step of the zenith angle is 1 degree and 5 degrees of the azimuth angle. The accuracy of the zenith and azimuth angle is 0.1 degree, and the relative error of the measured BRDF of the system is less than 5%. The reference-sample method [31] was used in the experiment. If  $f_{rs}(\theta_i, \varphi_i; \theta_r, \varphi_r)$  and  $f_{rr}(\theta_i, \varphi_i; \theta_r, \varphi_r)$  are the BRDF of the sample and the reflectance standard,

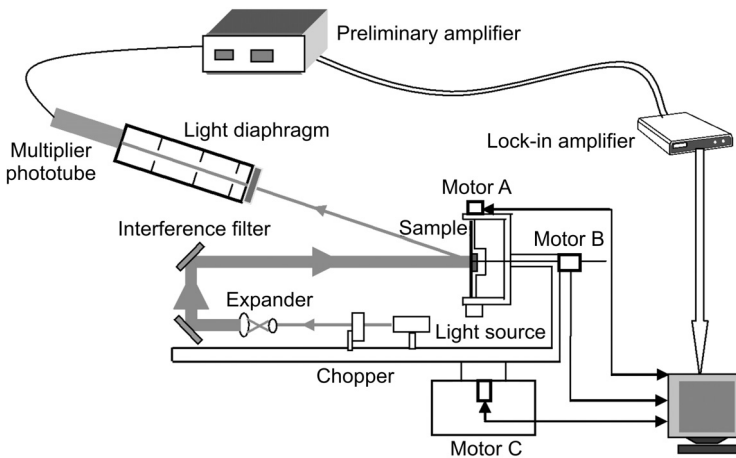


Fig. 3. Schematic of measurement instrument.

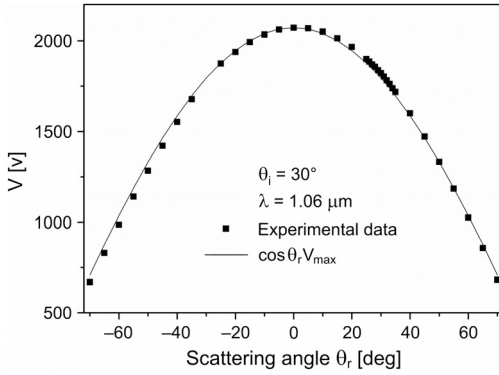


Fig. 4. Angular distribution of scattering intensity for the reference white plate (F4).

respectively, and if  $V_s$  and  $V_{\text{ref}}$  are the output voltages for the sample and the reflectance standard, respectively, then

$$\frac{f_{\text{rs}}(\theta_i, \varphi_i; \theta_r, \varphi_r)}{f_{\text{rr}}(\theta_i, \varphi_i; \theta_r, \varphi_r)} = \frac{V_s}{V_{\text{ref}}} \quad (7)$$

It is noticed that  $V_{\text{ref}}$  of the reference standard must be determined under the same measurement geometry conditions which are used for the detected samples and that all measurements must be performed in pairs. In our experiments, the reference standard is the pressed polytetrafluoroethylene plate which is considered as a Lambertian plate. Its scattering behavior closely approaches a perfectly diffuse, and the reflective spectra do not change at near-infrared bands. Figure 4 shows the output voltages that are corresponding to the angular distribution of backscattering intensity. The BRDF of a Lambert surface is a constant value in all directions, and the reference value is  $\rho/\pi$ , where  $\rho$  is the hemispherical reflectance using an optical spectrophotometer with an integration sphere. When the pressed polytetrafluoroethylene plate is used as a reference standard, its BRDF is  $f_{\text{rr}}(\theta_i, \varphi_i; \theta_r, \varphi_r) = \rho/\pi$ . Once the output voltages  $V_s$  and  $V_{\text{ref}}$  are measured, the BRDF of the target sample can be found. Thus the BRDF of the sample is:

$$f_{\text{rs}}(\theta_i, \varphi_i; \theta_r, \varphi_r) = \frac{V_s}{V_{\text{ref}}} f_{\text{rr}}(\theta_i, \varphi_i; \theta_r, \varphi_r) = \frac{V_s}{V_{\text{ref}}} \frac{\rho}{\pi} \quad (8)$$

#### 4. BRDF optimized modeling and verification

The surfaces of spatial targets are usually made of more than one material, as in the case of alloys and surface coatings containing random particles in a coating. By using the BRDF measurement system, we obtained the data of the isotropic surfaces in lab (the wavelength is 1.06  $\mu\text{m}$ ). The five-parameter model can be suitable for characterizing these surfaces by parameter optimization based on experimental data.

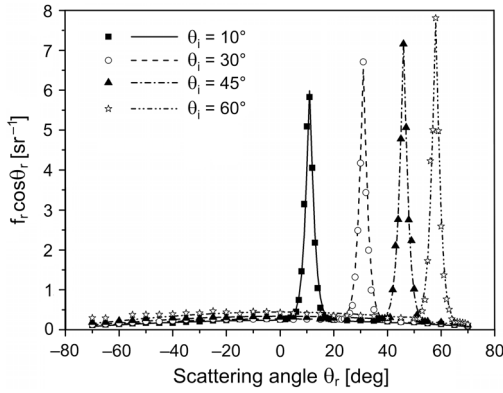


Fig. 5. BRDF of aluminum with coating of white paint (4 groups of data take part in fitting).

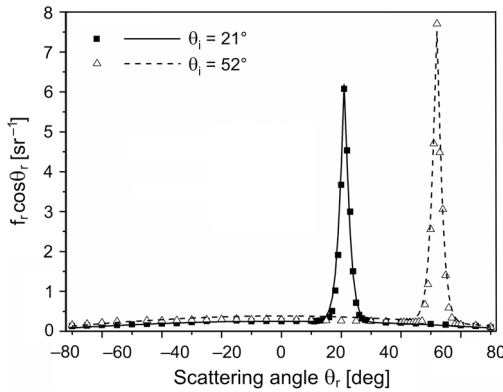


Fig. 6. BRDF of aluminum with coating of white paint (2 groups of data do not take part in fitting).

We measured 6 groups of data for the sample of aluminum with a coating of white (spray) paint, the incident angles are  $10^\circ$ ,  $30^\circ$ ,  $45^\circ$ ,  $60^\circ$ ,  $21^\circ$  and  $52^\circ$ , respectively. We choose 4 groups of data which take part in fitting, the incident angles are  $10^\circ$ ,  $30^\circ$ ,  $45^\circ$  and  $60^\circ$ . The other two groups of data (the incident angles are  $21^\circ$  and  $52^\circ$ , respectively) do not take part in fitting. Genetic algorithm is used in processing of optimized modeling. The five parameters are obtained by using genetic algorithm (GA), the parameters are  $k_b = 5.708$ ,  $k_r = 2.240$ ,  $b = -58.722$ ,  $a = 0.452$ ,  $k_d = 0.220$  and  $E = 4.17\%$ , where  $E$  is the error. The experimental data and fitted curves are shown in Fig. 5. The discrete points represent experimental data and the lines represent the fitted results. In Figure 6, the solid squares and hollow triangles are the experimental data for this sample which do not take part in fitting; the solid line and the dash line are calculated by Eq. (6) using the above five parameters. We can see that the five-parameter model can well predict the distribution of the light scattering.

As we know, directional hemisphere reflectance (DHR) is the integral of BRDF over the upper hemisphere [7]:

$$\rho = \int_{2\pi} f_r \cos \theta_r \, d\omega_r \quad (9)$$

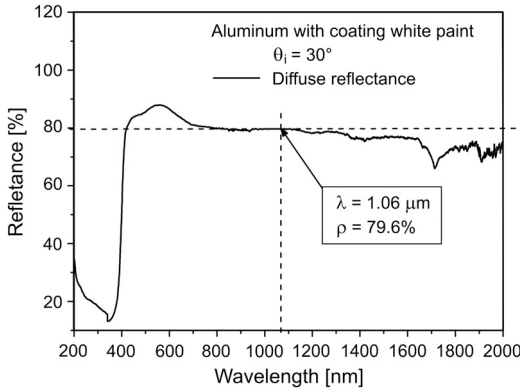


Fig. 7. The reflectance of aluminum with coating of white paint.

The measured hemispherical reflectance of this sample from 200 nm to 2000 nm (by using a spectrophotometer (U-3501) with integrating sphere) is shown in Fig. 7. We can see, when the wavelength is 1.06  $\mu\text{m}$ , that the value is 79.6%.

With the equation above, we can obtain the value of the reflectance  $\rho$  is 73.4%, which closes to the value 79.6%, which is measured by integral sphere, while is relatively accurate. This means that the experimental method and the model presented in this paper are applicable.

## 5. BRDF statistical models of various samples

The five-parameter model can fit many kinds of surfaces, several samples of BRDF are shown in this section.

### 5.1. Cement plate

The roughness of the cement plate surface is very large. When the five-parameter model is applied to this kind of a plane, the light scattering characteristics are the same as that of a Lambertian plane. The specular component is almost zero. The five parameters are  $k_b = 0.003$ ,  $k_r = 2.961$ ,  $b = -18.301$ ,  $a = 15.572$ ,  $k_d = 0.067$  and  $E = 5.98\%$ . The experimental data and fitted curves are shown in Fig. 8. The Figure 9 shows the 3D spatial distribution of  $f_r(\theta_i; \theta_r, 0)\cos\theta_r$  changing with  $\varphi_r, \theta_r$ .

### 5.2. Forged steel with coating of khaki paint and forged steel

For a surface of forged steel with coating of khaki paint, the parameters are given as  $k_b = 0.0698$ ,  $k_r = 0.478$ ,  $b = -28.935$ ,  $a = 0.777$ ,  $k_d = 0.107$  and  $E = 0.69\%$ . The simulated curves are shown in Fig. 10. The 3D BRDF is shown in Fig. 11.

For a surface of forged steel, the parameters are  $k_b = 0.072$ ,  $k_r = 16.125$ ,  $b = -29.917$ ,  $a = 0.959$ ,  $k_d = 0.081$  and  $E = 0.95\%$  can be obtained from the five-parameter model. Figure 12 shows experimental BRDF data and the fitted curves.



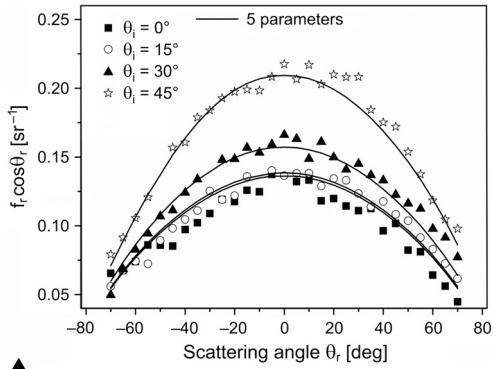


Fig. 8. BRDF of cement plate.

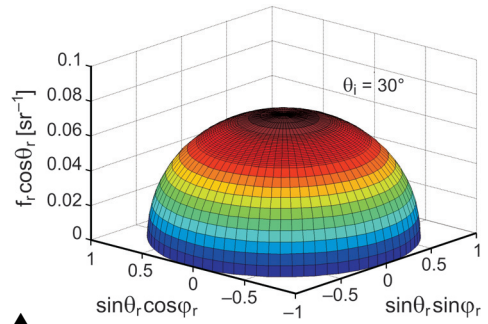


Fig. 9. 3D BRDF of cement plate.

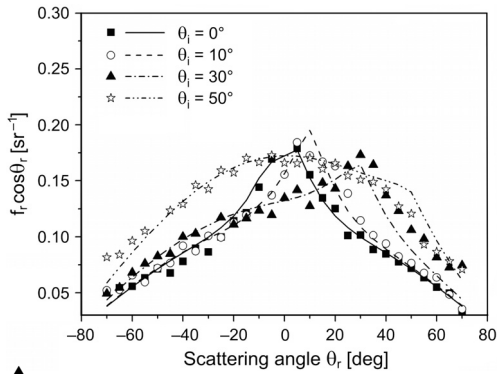


Fig. 10. BRDF of forged steel with coating khaki paint.

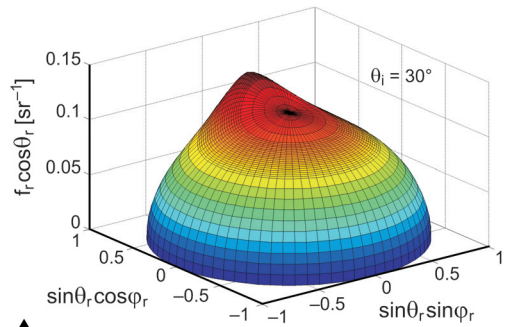


Fig. 11. 3D BRDF of forged steel with coating khaki paint.

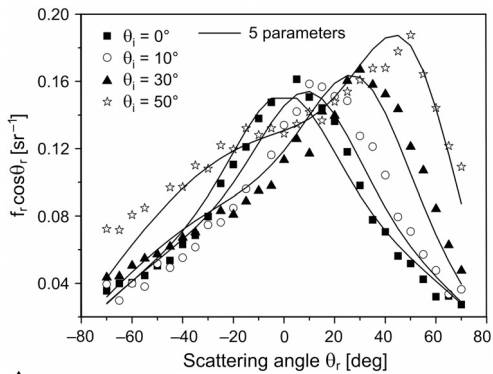


Fig. 12. BRDF of forged steel.

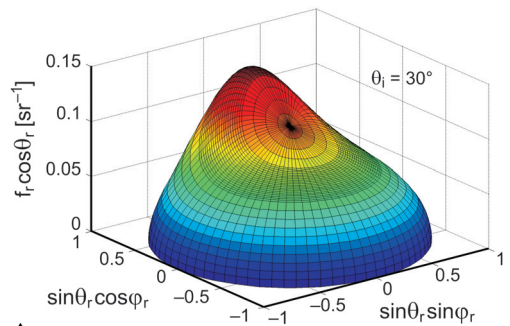
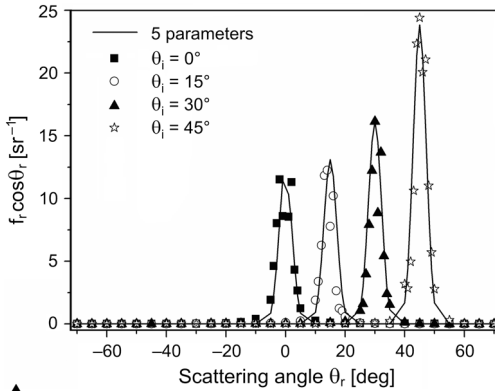
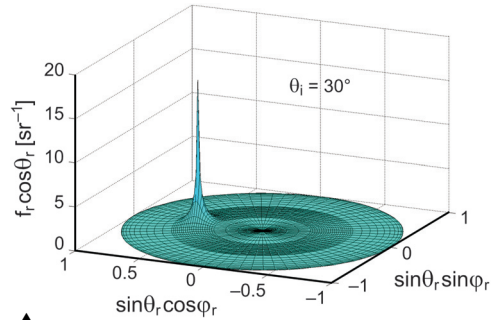


Fig. 13. 3D BRDF of forged steel.



▲ Fig. 14. BRDF of polyimide film.



▲ Fig. 15. 3D BRDF of polyimide film.

It shows us that the model can fit the experimental data well. Figure 13 shows the 3D BRDF distribution.

### 5.3. The surface of polyimide film

The sample of polyimide film is very glossy. The specular peak is obvious and the five-parameters can be fitted well. The five parameters are  $k_b = 5.439$ ,  $k_r = 3.257$ ,  $b = -23.098$ ,  $a = 0.495$ ,  $k_d = 2.267$  and  $E = 10.1\%$ . The experimental data and fitted curves are shown in Fig. 14. Figure 15 is the 3D BRDF of a polyimide film.

## 6. Conclusions

A modified BRDF model, a five-parameter model, is proposed. It is based on the Torrance–Sparrow model, and a detailed discussion of this model is also given. BRDF of five samples with different surface optical properties is measured in the laboratory. The five-parameter model is used to fit the experimental data. Genetic algorithm is used to search the best parameters of the model. It is shown that the five-parameter model is applicable to different kinds of material roughness and optical characteristics. The five-parameter model avoids the difficulties of obtaining the surface roughness and optical constants of materials for precise theoretical analysis, and gives us more information on target surface scattering. The method has a promising application in earth surface BRDF modeling.

*Acknowledgements* – This work was supported by the National Natural Science Foundation of China (NSFC) (No. 60771038), and the Fundamental Research Funds for the Central Universities.

## References

- [1] ABD-EL-RAOUF H.E., MITTRA R., *Scattering analysis of dielectric coated cones*, Journal of Electromagnetic Waves and Applications **21**(13), 2007, pp. 1857–1871.

- [2] CHEN K.S., FUNG A.K., SHI J.C., LEE H.W., *Interpretation of backscattering mechanisms from non-Gaussian correlated randomly rough surfaces*, Journal of Electromagnetic Waves and Applications **20**(1), 2006, pp. 105–118.
- [3] FUNG A.K., KUO N.C., *Backscattering from multi-scale and exponentially correlated surfaces*, Journal of Electromagnetic Waves and Applications **20**(1), 2006, pp. 3–11.
- [4] NISHIMOTO M., UENO S., KIMURA Y., *Feature extraction from GPR data for identification of landmine-like objects under rough ground surface*, Journal of Electromagnetic Waves and Applications **20**(12), 2006, pp. 1577–1586.
- [5] OHNUKI S., CHEW W.C., HINATA T., *Monte Carlo simulation of 1-D rough surface scattering in 2-D space*, Journal of Electromagnetic Waves and Applications **19**(8), 2005, pp. 1085–1102.
- [6] STRIFORS H.C., GAUNAURD G.C., *Bistatic scattering by bare and coated perfectly conducting targets of simple shape*, Journal of Electromagnetic Waves and Applications **20**(8), 2006, pp. 1037–1050.
- [7] NICODEMUS F.E., *Reflectance nomenclature and directional reflectance and emissivity*, Applied Optics **9**(6), 1970, pp. 1474–1475.
- [8] ZHANG Y.Q., WU Z.S., *Character of light scattering of spatial dynamic objects at different stations and analysis of relativity*, Journal of Electromagnetic Waves and Applications **22**(8–9), 2008, pp. 1071–1080.
- [9] GIBBS D.P., BETTY C.L., FUNG A.K., BLANCHARD A.J., IRONS J.R., BALSAM W.L., *Automated measurement of polarized bidirectional reflectance*, Remote Sensing of Environment **43**(1), 1993, pp. 97–114.
- [10] DITTMAN M.G., *K-correlation power spectral density and surface scatter model*, Proceedings of SPIE **6291**, 2006, p. 62910R.
- [11] LATIFOVIC R., CIHLAR J., CHEN J., *A comparison of BRDF models for the normalization of satellite optical data to a standard Sun-target-sensor geometry*, IEEE Transactions on Geoscience and Remote Sensing **41**(8), 2003, pp. 1889–1898.
- [12] MEISTER G., WIEMKER R., MONNO R., SPITZER H., STRAHLER A., *Investigation on the Torrance–Sparrow specular BRDF model*, [In] *Geoscience and Remote Sensing Symposium Proceedings (IGARSS'98)*, Vol. 4, IEEE International, 1998, pp. 2095–2097.
- [13] SANDMEIER S., SANDMEIER W., ITTEN K.I., SCHAEPMAN M.E., KELLENBERGER T.W., *Acquisition of bidirectional reflectance data using the Swiss Field-Goniometer System (FIGOS)*, [In] *Proceedings of EARSeL Symposium*, Basel, Switzerland, Balkema, Rotterdam, 1995, pp. 55–61.
- [14] SANDMEIER S., MÜLLER C., HOSGOOD B., ANDREOLI G., *Sensitivity analysis and quality assessment of laboratory BRDF data*, Remote Sensing of Environment **64**(2), 1998, pp. 176–191.
- [15] PAPETTI T.J., WALKER W.E., KEFFER C.E., JOHNSON B.E., *Coherent backscatter: measurement of the retroreflective BRDF peak exhibited by several surfaces relevant to lidar applications*, Proceedings of SPIE **6682**, 2007, p. 66820E.
- [16] VOSS K.J., CHAPIN A., MONTI M., ZHANG H., *Instrument to measure the bidirectional reflectance distribution function of surfaces*, Applied Optics **39**(33), 2000, pp. 6197–6206.
- [17] ZHANG H., VOSS K.J., *Comparisons of bidirectional reflectance distribution function measurements on prepared particulate surfaces and radiative-transfer models*, Applied Optics **44**(4), 2004, pp. 597–610.
- [18] WOLFF L.B., *Diffuse-reflectance model for smooth dielectric surfaces*, Journal of the Optical Society of America A **11**(11), 1994, pp. 2956–2968.
- [19] CULPEPPER M.A., *Empirical bidirectional reflectivity model*, Proceedings of SPIE **2469**, 1995, pp. 208–219.
- [20] ICART I., ARQUES D., *Simulation of the optical behavior of rough identical multilayers*, Proceedings of SPIE **4100**, 2000, pp. 84–95.
- [21] WATSON R.M.J., RAVEN P.N., *Comparison of measured BRDF data with parameterized reflectance models*, Proceedings of SPIE **4370**, 2001, pp. 159–168.
- [22] STARK M.M., ARVO J., SMITS B., *Barycentric parameterizations for isotropic BRDFs*, IEEE Transactions on Visualization and Computer Graphics **11**(2), 2005, pp. 126–138.

- [23] GERMER T.A., ASMAIL C.C., *Goniometric optical scatter instrument for bidirectional reflectance distribution function measurements with out-of-plane and polarimetry capabilities*, Proceedings of SPIE **3141**, 1997, pp. 220–231.
- [24] GERMER T.A., *Application of bidirectional ellipsometry to the characterization of roughness and defects in dielectric layers*, Proceedings of SPIE **3275**, 1998, pp. 121–131.
- [25] PRIEST R.G., GERMER T.A., *Polarimetric BRDF in the microfacet model: Theory and measurements*, [In] *Proceedings of the 2000 Meeting of the Military Sensing Symposia Specialty Group on Passive Sensors*, Infrared Information Analysis Center, Ann Arbor, MI, 2000, pp. 169–181.
- [26] GERMER T.A., *Polarized light diffusely scattered under smooth and rough interfaces*, Proceedings of SPIE **5158**, 2003, pp. 193–204.
- [27] GERMER T.A., *Measuring interfacial roughness by polarized optical scattering*, [In] *Light Scattering and Nanoscale Surface Roughness*, [Ed] A.A. Maradudin, Springer, 2006, pp. 259–284.
- [28] MARSCHNER S.R., WESTIN S.H., LAFORTUNE E.P.F., TORRANCE K.E., GREENBERG D.P., *Image-based BRDF measurement including human skin*, [In] *10th Eurographics Workshop on Rendering*, 1999.
- [29] TORRANCE K.E., SPARROW E.M., *Theory for off-specular reflection from roughened surfaces*, Journal of the Optical Society of America **57**(9), 1967, pp. 1105–1112.
- [30] ZHOU M., SUN S., *Algorithms Theory and Applications*, National Defence Industry Press, Beijing, 1997.
- [31] BARTELL F.O., DERENIAK E.L., WOLFE W.L., *The theory and measurement of bidirectional reflectance distribution function (BRDF) and bidirectional transmittance distribution function (BTDF)*, Proceedings of SPIE **257**, 1981, pp. 154–160.

*Received May 29, 2009  
in revised form August 1, 2009*